Rev.Adv.Mater.Sci. 5 (2003) 6-16

SUPERHARD AND FUNCTIONAL NANOCOMPOSITES FORMED BY SELF-ORGANIZATION IN COMPARISON WITH HARDENING OF COATINGS BY ENERGETIC ION BOMBARDMENT DURING THEIR DEPOSITION

Stan Veprek

Institute for Chemistry of Inorganic Materials, Technical University Munich, Lichtenbergstr. 4, D- 85747 Garching b. Munich, Germany

Received: June 25, 2003

Abstract. Since the publication of our generic concept for the design of novel superhard nanocomposites, a number of superhard and functional nanocomposites of different composition were prepared and investigated. The nc-$(Al_{1-x}Ti_x)N$/a-Si_3N_4 nanocomposite coatings for wear protection of machining tools for dry and fast cutting as well as the new coating technology needed for their large scale industrial production were successfully developed and introduced on the market.

In the first part we shall briefly discuss the different approaches to the preparation of superhard coatings including the hardening by energetic ion bombardment during the deposition. This includes a variety of ordinary hard coatings, such as TiN, (Ti,Al,V)N, HfB_2 and also the so called "nanocomposites" consisting of a hard transition metal nitride and a soft, ductile metal which does not form any stable nitride, e. g. ZrN/Ni, CrxN/Ni, ZrN/Cu, TiN/Cu. As there is no evidence of a contribution to the hardening by a nanostructure in these coatings, the stability of their hardness is limited to 400-600 °C.

The second part deals with the present status of our understanding of the formation of thermally very stable (≥1100 °C), superhard nanostructures by self-organization as a result of thermodynamically driven spinodal phase segregation. We discus the recent progress in the understanding of the extraordinary combination of their mechanical properties, such as high hardness of 40-100 GPa combined with a high elastic recovery of 80-95 % and a high resistance against brittle failure by catastrophic crack initiation and propagation. The tensile strength of the super- and ultrahard nanocomposites prepared in this way reaches 10-40 GPa approaching the ideal cohesive strength of strong solids. These properties can be relatively easily understood in terms of conventional fracture physics scaled down to crystallite size of few nanometers and accounting for the critical activation volume needed for the initiation of plastic deformation and structural transitions.

1. INTRODUCTION

Superhard materials with Vickers hardness $H_V \geq 40$ GPa received recently increasing attention because of their already existing and potential future applications, e. g. as protective tribological coatings for machining and forming tools. The intrinsically superhard materials include diamond ($H \approx 70-90$ GPa; industrial diamonds may have a higher hardness due to substitutionally dissolved nitrogen) and cubic boron nitride c-BN ($H \approx 48$ GPa). Their application as protection coatings is still limited. Therefore we shall, in the present paper, concentrate on extrinsically superhard materials briefly summarizing the recent progress that was achieved in their preparation, in the understanding of their thermal stability and mechanical properties and in industrial applications.

Corresponding author: Stan Veprek, e-mail: Veprek@ch.tum.de

One might ask how is it possible to prepare materials with hardness approaching or even reaching that of diamond. The answer is quite simple: The presence of flaws, such as dislocations and microcracks, in engineering materials limits their strength to a small (10^{-4}–10^{-2}) fraction of their ideal strength. The latter can be estimated as about $0.1 \cdot G$ for materials which display crystal plasticity and about $(0.1\text{-}0.2) \cdot E_Y$ for glasses where dislocations are absent. (G and E_Y are the shear and Young's modulus, respectively.) Thus, the ideal strength of intrinsically strong materials lies in the range of several 10 GPa but their practicably achievable one seldom exceeds several 100 MPa. Furthermore, conventional hard materials are brittle and have a small elastic limit of ≤ 0.1% above of which fracture occurs. Therefore, the strengthening of conventional engineering materials is based on an appropriate engineering of the microstructure that hinders the formation and propagation of flaws. In spite of that, the strength of the strongest steels and metallic alloys in bulk reaches only 1–2 GPa and their elastic limit is below 0.5%. The upper limit of tensile strength of ≤ 2 GPa and elastic range of ≤ 2% was achieved in some metallic glasses.

With the decrease of the size of the tested specimen, the probability of the occurrence of a critical flaw which limits its strength decreases and its strength increases accordingly. This has been reported by Leonardo da Vinci who found that the strength of iron wires decreases with their increasing length ([1] and references therein). In his classical paper, Griffith [2] reported on the strength of freshly drawn SiO_2 fibres that reached values of about 10 GPa, close to the ideal one. He also noticed that the strength strongly decreased after a short exposure to air approaching the value of only several 100 MPa after one day. This is due to the chemical attack of the surface of the fibres by H_2O that inserts into the strongly polar Si-O bonds causing their breaking which results in the nucleation of surface microcracks. Nowadays it is well established, that the strength of very thin wires and fibres can reach high values of tens of GPa thus approaching the ideal strength (≤ 5 GPa for 100 μm thin steel wires, up to 20 GPa for 0.05 – 0.26 μm thin W-wires and similar for a variety of whiskers [3]). When freshly drawn and immediately measured under vacuum, SiO_2 glass fibres reach tensile strength of 15 GPa corresponding to about 21% of the Young's modulus [3].

Based on this knowledge it is obvious that the logical strategy towards the design of strong (and superhard) materials is to make them free of flaws. Because the conventional preparation techniques used in materials manufacturing, such as the control of a small grain size ('Hall-Petch' relationship), solution and precipitation hardening, consolidation of nanopowders and densification of the grain boundaries in order to minimize the grain boundary sliding by the sintering of fine-grain ceramics and others, cannot control the random occurrence of flaws, new techniques which involve some kind of self-organization of the nanostructure are the logical way to follow. This is the basis of our generic concept for the design of superhard nanocomposites in which the self-organization is achieved by a strong, thermodynamically driven, spinodal segregation in binary (or ternary) phase system [4, 5].

Work hardening is a complex phenomena frequently used for strengthening of materials. In a very simplified manner it is related to the repulsive interaction between intersecting dislocations. Hall and Petch have shown that based on the confinement of dislocation pile-ups into smaller regions the yield stress of a polycrystalline material increases proportionally to the decrease of the square root of the crystallite size d, $\sigma_Y = \sigma_0 + k/\sqrt{d}$ [6,7]. Accordingly, the well known and frequently used hardening of materials due to decreasing crystallite size is called the 'Hall-Petch' effect although in many cases the mechanism may be quite different. For example, in fine grain nanocrystalline ceramics that show no dislocation activity, the strength is limited by catastrophic growth of critical microcracks, a flaw remaining between the grains after a non-ideal sintering. Because the size of such microcrack, a, scales with that of the grains, d, and because the critical stress for the catastrophic growth of such a microcrack is proportional to the $1/\sqrt{a}$ (Griffith criterion [1, 2]), one finds an experimental relationship between the strength and crystallite size similar to the Hall-Petch relationship. Thus, a phenomenologically similar strengthening with decreasing grain size is found also for fine grain brittle materials as described by the Hall-Petch relationship for ductile metals which undergo crystal plasticity. With this in mind, smaller crystallite size and work hardening in general sense result in an increase of the strength (and hardness) of both ductile metals and brittle ceramics. The decreasing crystallite size upon energetic ion bombardment is one part of the synergistic effect that yields the hardness enhancement found in thin coatings consisting of ordinary hard materials when they are deposited under energetic ion bombardment. This is discussed in the next section.

2. DIFFERENT WAYS TOWARDS SUPERHARD COATINGS

The considerations outlined in the previous section as well as a survey of the current literature [8-12] allows us to identify three different approaches towards the preparation of superhard coatings: 1) Deposition of intrinsically superhard materials, such as diamond and c-BN in a kinetically controlled regime, 2) hardening due to energetic ion bombardment during the deposition and 3) formation of an appropriate nanostructure which hinders the formation and propagation of flaws.

The deposition of diamond and c-BN has been reviewed by many authors (see e.g. [11] and references therein) and, therefore, will not be discussed here because so far, the applications of these coatings are limited. The nanostructured superhard coatings include the heterostructures and nanocomposites. The preparation and properties of heterostructures are well established and described in a large number of papers. Therefore we shall not discuss them here and refer to the relevant reviews [8, 10, 11] and original papers quoted there.

2.1. Energetic ion bombardment of the surface of the growing film can be easily achieved in a variety of glow discharge, low pressure plasma PVD (non-reactive and reactive sputtering, vacuum arc evaporation, reactive activated evaporation and ion plating [13]) and in plasma CVD. The energy of the ions impinging on the surface is controlled by the difference between the electric potential of that surface and that of the plasma, and by the total gas pressure and its composition. It can vary between about 10 eV when the substrate is floating and several 100 eV when it is appropriately biased and the gas pressure is low so that the mean free path of the ions is larger than the thickness of the space charge sheath between the substrate and the quasi-neutral plasma. Because the exact measurement of the ion energy is a relatively difficult task, its value is either unknown or only roughly estimated in the majority of the papers reporting on the preparation of coatings. (Notice, that in the majority of the papers the author report the "substrate bias" measured with respect to ground, but the plasma potential, whose difference to that of the substrate determines the actual value of the bias, is unknown.)

The effect of energetic ion bombardment on the properties of deposited coatings is complex as demonstrated, for example, by the nc-Si deposited by means of chemical transport in hydrogen plasma [14]. In this experiment, the energy of the H^+ ions, which are dominating the observed effects, scales approximately with the substrate bias. It was shown that already at a low ion energy of ≤ 100 eV the crystallite size strongly decreases and a high biaxial compressive stress is build-up in the film with increasing ion flux and energy reaching values of 4 – 6 GPa. Starting from the threshold energy of 117 eV for the displacement damage in silicon by H^+ ions, defect formation is seen in the one-phonon density-of-state absorption spectra that results in amorphisation of the film at high ion energies of ≥ 700 eV [14]. (Notice that the threshold energy for radiation damage depends on the ratio of the mass of the primary ion and that of the atoms of the growing film; it is smaller for heavier ions, such as Ar^+.) The high compressive stress results also in a densification of the grain boundaries that hinders the grain boundary sliding which otherwise results in a decrease of the hardness when the crystallite size decreases below about 6 – 10 nm.

Reactive sputtering at low pressure of the order of 10^{-3} mbar, particularly when unbalanced magnetron is used, is a typical example of the deposition of coating under such bombardment by the primary energetic ions reflected from the target, even without an externally applied bias to the substrate. It is therefore the most appropriate technique to achieve superhardness in ordinary coatings as demonstrated by many researchers. Musil *et al*. reported hardness of 100 GPa for (TiAlV)N and 80 GPa for TiN [15] and Herr and Broszeit found hardness of 70 GPa for HfB_2 [16]; the bulk hardness of all these materials amounts to 18-25 GPa only. In the latter case, the researchers also determined the biaxial compressive stress in the coatings of –7 GPa which however, upon annealing to ≥ 400 °C relaxed and the hardness decreased to the ordinary value of ≤ 20 GPa.

A similar relaxation of the hardness and stress upon annealing to ≤ 400 °C was reported [17] also for the "superhard nanocomposites" consisting of a hard transition metal nitride and a few at.% of a ductile metal which does not form stable nitrides, as prepared and reported in many papers by Musil *et al*. [18]. Fig. 1 shows an example of the behavior of these coatings upon annealing [17, 19]. The decrease of the hardness (Fig. 1a) is accompanied by a relaxation of the biaxial stress (Fig. 1c). Of course, the annealing results also in vanishing of the ion bombardment induced defects that cause the hardness enhancement whereas the crystallite size remains unchanged (Fig. 1b). Therefore, the enhancement of the hardness observed in these coatings is

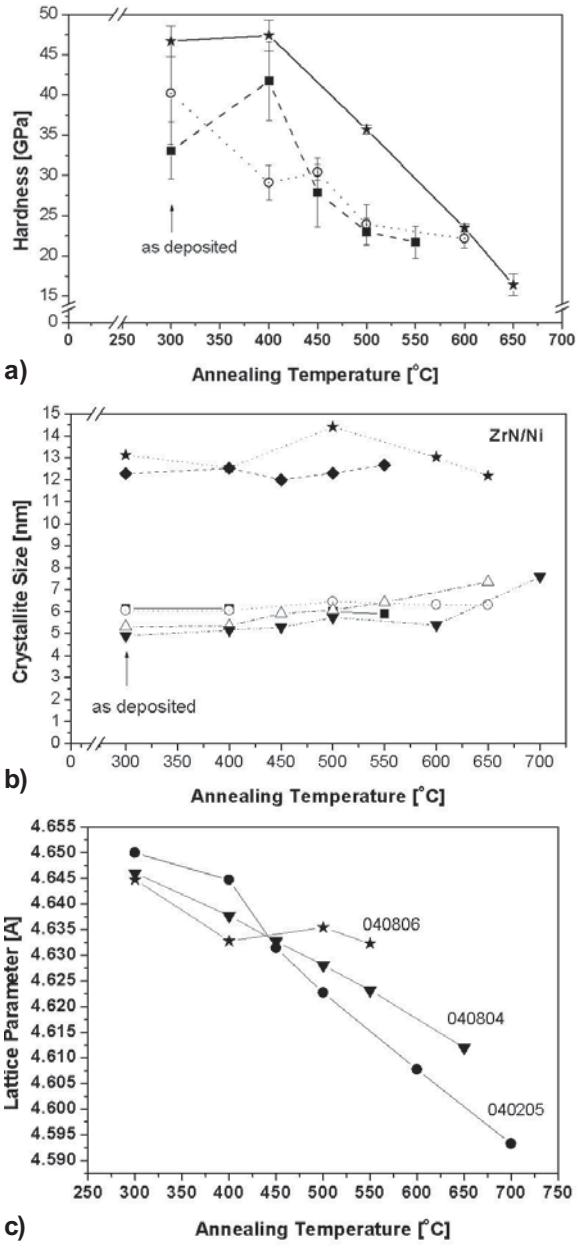

Fig. 1. a): Decrease of the hardness of three samples of ZrN/Ni coatings, deposited by Musil *et al.* by means of unbalanced magnetron at low pressure at substrate temperature of 300 °C, upon annealing, when the crystallite size remains unchanged (Fig. b for a total of 6 coatings including those in Fig. a) but the biaxial compressive stress relaxes (Fig. c) [17].

evidently due to the energetic ion bombardment and not to any effect of the "nanostructure".

The relatively low thermal stability of the hardness enhancement due to the "work hardening" induced by the energetic ion bombardment is a logical consequence of the low thermal stability of the induced defects. It will be shown later, that the high hardness of the superhard nanocomposites consisting of immiscible hard transition metal nitrides (TiN, $(Al_{1-x}Ti_x)N$, W_2N, VN and others) in combination with a covalent nitride (e. g. Si_3N_4, BN) either remains constant or even increases upon annealing up to 1000 – 1100 °C.

2.2. Superhard nanocomposites formed from immiscible hard materials, such as transition metal nitrides in combination with covalent refractory nitrides by self-organization upon a strong thermodynamically driven segregation [4, 5, 11] show a much higher thermal stability because any coarsening of the segregated phases upon annealing requires a high activation energy. This is a consequence of the fact that for a system which undergoes spinodal decomposition the second derivative of the Gibbs free energy of the mixed phase with an infinitesimal, local change of the composition is negative [5, 20, 21]. Thus the Ostwald ripening is hindered by the absence of any reaction at the interface [20, 21], i.e. by the lack of solubility. In contrast, any infinitesimal change of the composition of the mixed phase upon spinodal decomposition leads to a decrease of the Gibbs free energy of the system and, therefore, it proceeds without any activation up to the formation of the final fully segregated nanostructure which is characterized by a sharp boundary between the phases and a fairly regular spatial periodicity (crystallite size) in nanometer range. The characteristic size of the self-organized nanostructure is given by a balance between the decrease of the Gibbs free energy of the segregation, the destabilizing term corresponding to the elastic lattice energy due to incoherency of the interface and term due to chemical gradients [4, 20, 21-24].

The high thermal stability of our nanocomposites prepared according to this principle was documented by a number of examples in recent papers [5, 25]. In Fig. 2 we show two examples of the high temperature behavior of nc-TiN/a-Si_3N_4 deposited by plasma CVD in a laboratory equipment and nc-$(Al_{1-x}Ti_x)N$/a-Si_3N_4 coatings which are now available on a large industrial scale [26, 27]. Both coatings remain stable upon annealing up to ≥ 1100 °C. The example of the nc-$(Al_{1-x}Ti_x)N$/a-Si_3N_4 industrial coatings is of a substantial interest and practical importance because it shows that the formation of the stable nanocomposite in which the $(Al_{1-x}Ti_x)N$ nanocrystals are separated by immiscible a-Si_3N_4 tissue hinders the decomposition and softening of $(Al_{1-x}Ti_x)N$. The metastable fcc $(Al_{1-x}Ti_x)N$ decomposes to the fcc TiN

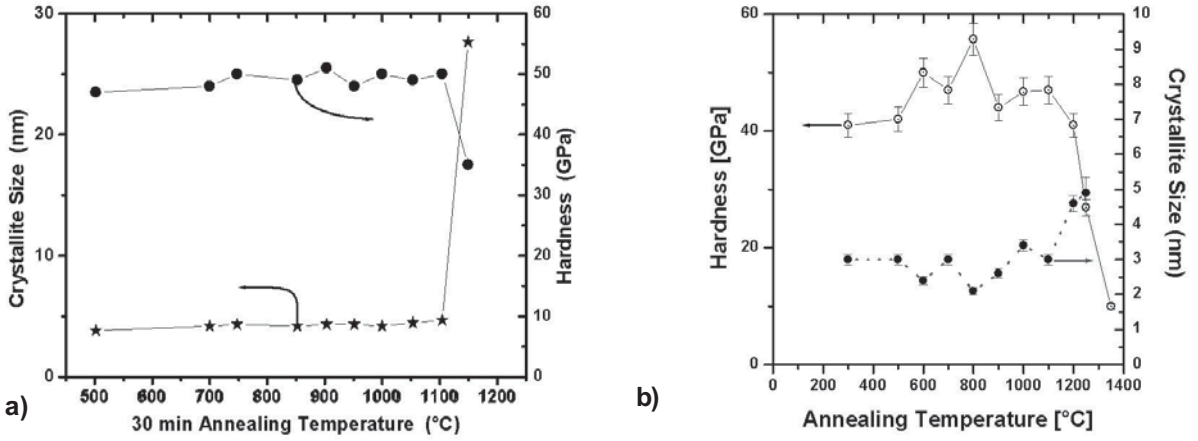

Fig. 2. Example of annealing behavior of nc-TiN/a-Si_3N_4 superhard nanocomposites deposited by plasma CVD in a laboratory equipment (Fig. a) and of nc-$(Al_{1-x}Ti_x)N$/a-Si_3N_4 coatings deposited by means of vacuum arc evaporation on cemented substrate at a temperature of about 450 °C. It is seen that these coatings show a much higher thermal stability up to 1200 °C. Notice, that the decomposition of the fcc $(Al_{1-x}Ti_x)N$ to fcc TiN and h AlN, that usually occurs at a temperature of ≤ 900 °C resulting in softening of the coatings, is absent (see text).

and h AlN at ≤900 °C which is accompanied by softening which limits the temperature range of the applications of the conventional $(Al_{1-x}Ti_x)N$ coatings [28, 29]. The $(Al_{1-x}Ti_x)N$/a-Si_3N_4 superhard nanocomposites are stable to much higher temperatures where a strong diffusion of cobalt from the cemented carbide substrate limits the stability of the coated tools [30-35].

3. MECHANICAL PROPERTIES OF SUPERHARD NANOCOMPOSITES

As already mentioned above, the hardness enhancement in coatings deposited under energetic ion bombardment is due to combined effects of the decrease of the crystallite size, densification of the grain boundaries, 'work hardening' due to the formation of defects which hinder flaws (dislocations and microcracks) to grow and propagate, large biaxial stress and possibly others. The understanding of these complex effects is still in its infancy [18]. For this reason and because of their low thermal stability, no industrial application was reported so far, we shall not discuss them here.

Much progress was achieved in the understanding of the mechanical properties [22–24] of the superhard nanocomposites prepared according to the generic principle by spinodal phase segregation [4, 5]. It has been shown that their unusual combination of high hardness of 40 to 100 GPa, high elastic recovery of 80 to 94% and high tensile strength of several 10 GPa upon indentation can be relatively easily understood on the basis of conventional fracture physics scaled down to a size of few nanometer corresponding to the size of the nanocrystals. The key for the achieving of these properties is the stable nanostructure which is essentially free of flaws when formed by the self-organization upon the spinodal phase segregation. Fig. 3a shows an example of the hardness measured vs. the applied load on a 3.5 μm thick ultrahard ternary nc-TiN/a-Si_3N_4/a-$TiSi_2$ nanocomposite with a hardness of about 105 GPa in comparison with that of a thin nc-Diamond coatings and with a bulk industrial diamond. One can see that hardness indeed exceeds 100 GPa. Of course, hardness measurements in such range can be subject to a number of artifacts that may yield an apparently too high values (see [24, 36]). One can see that the measurements shown in Fig. 3, which clearly show the range of load-independent hardness of the coatings, that was also checked by calibrated SEM give reliable values. We emphasize this point here because these data were recently questioned by some workers (see [37] and reply [38]).

Fig. 3b shows an example of the indentation curve measured on such coatings. It is seen that the ultrahard coating shows upon indentation a high elastic recovery of 94%. The remaining plastic indentation is free of any cracks although the indentation depth exceeds 10% of the thickness of the coatings. Even at the highest load of 1000 mN no

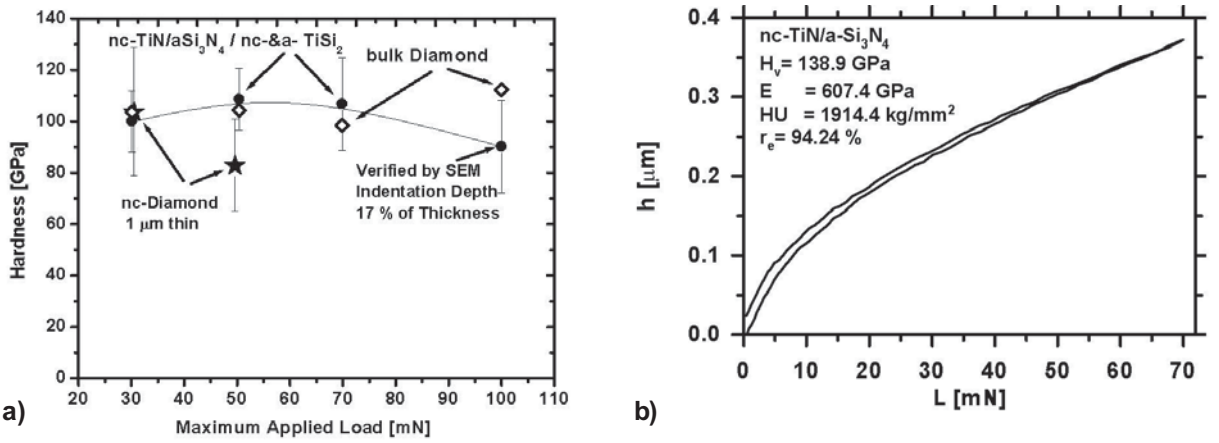

Fig. 3. a) Hardness of ultrahard nc-TiN/a-$_3$N$_4$/a- & nc-TiSi$_2$ nanocomposites vs. the applied load in comparison with hardness of nc-Diamond coatings and with bulk industrial diamond. b) Example of a typical indentation curve found in the measurements on super- and ultrahard nanocomposites that shows a high elastic recovery and reversibly stored (elastic) energy.

crack formation is observed (for further details see [24]). Furthermore, from the indentation curve shown in Fig. 3b we estimated the recoverably stored (elastic) energy density of ≥ 3 kJoule/mole which is an order of magnitude larger than elastic energy which can be stored upon a large strain of 1% in a strong ceramic material like the hard transition metal nitrides [22, 23]. Because conventional hard materials are brittle and sustain only a small strain of $\leq 10^{-3}$ and even ductile metals have elastic limits of the order of 10^{-3} which can accommodate only a small elastic energy, the question arises as to how can we understand such an unusual combination of properties. These questions were discussed in our recent papers [22–24]. Here we summarize the most important findings:

Because dislocation activity is absent in nanocomposites with a crystallite size of ≤ 10-20 nm, the high hardness can be easily understood in the context of the brittle failure of ceramics and glasses. Because of the absence of critical flaws outlined above, the maximum size of voids ("nanocracks") which might be present in such materials is of the order of 1-2 nm which results in a very small stress concentration factor of 2 to 4 as compared to 30 to 100 in fine grain submicron ceramics. Thus, the nanocomposites should approach the ideal cohesive strength of the hard ceramic nitrides [23] which is of the order of several 10 GPa [22].

Hertzian analysis of the unloading curves of many indentations (see [22-24]) confirmed that the response is indeed truly elastic although the material under the indenter operates in a highly non-linear regime, i. e. Hooke's law with a constant elastic modulus does not apply [22]. The experimental finding according to which these materials sustain a large strain far within the non-linear regime without fracture in which a very large energy is reversibly stored was explained in terms of flexing which is illustrated in Fig. 4 [23]. The universal decohesion curve (Fig. 4a) shows that an interatomic bond can sustain a large dilatation $100\cdot(a_{max}-a_0)/a_0$ of up to 20% and still recover reversibly whereas a bulk, brittle material will undergo fracture at a strain of ≤0.1 %. Thus, an order of magnitude larger energy can be reversible stored in this non-linear elastic deformation as shown in Fig. 4b [23].

The loading indentation curve, Hertzian analysis and SEM micrographs were used to verify the absence of crack formation in the indentation in a series of super- and ultrahard coatings. It was found that the coatings sustain up to 20% strain (at the microscopic scale) without cracking [24]. This can be understood in terms of the absence of critical flaws: Considering the stress intensity factor $K_1 = \sigma\sqrt{\pi a_{Crack}}$, which is the conventional measure of fracture toughness, it is obvious that for $a_{Crack} \approx$ 1-2 nm small nanocracks in the nanocomposites an order of magnitude higher stress σ is needed to induce their propagation as compared with a fine grain, submicroscopic ceramics ($a_{Crack} \approx$ 100-200 nm) even if the stress intensity factor were the same in both materials [23]. Thus, the very high resistance of the nanocomposites against failure by catastrophic crack is due to a high stress needed for the crack initiation and not –

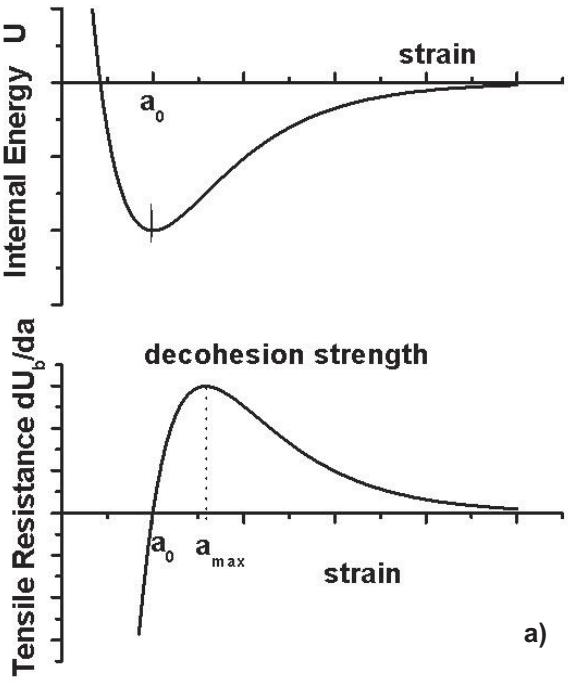

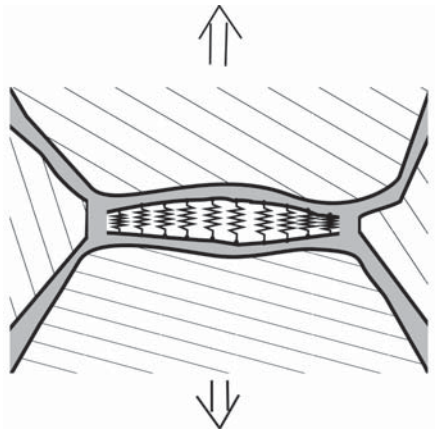

Fig. 4. a) Internal energy vs. tensile strength (above) and the first derivative (below) which corresponds to the restoring force acting between interatomic bonds upon strain ("universal decohesion curve"). b) Flexing – reversible dilatation within the non-linear regime of the universal decohesion curve for dilatation between a_0 and a_{max}.

as often incorrectly stated – to a high fracture toughness.

After having proven that our nanocomposites sustain such high and primarily elastic deformation without fracture we could estimate the maximum tensile stress that occurs upon the indentation at the periphery of the contact between the coatings and the indenter. Hertzian theory yields a simple analytical equation which was used to calculate the value of this strain [22, 23]. This value is a lower limit of the tensile strength of the nanocompositess. Evaluation of experimental indentations for a series of ultra- and superhard coatings reveals that their tensile strength reaches several 10 GPa as shown in Fig. 5 [24], thus approaching the ideal cohesive strength of flaw-free strong materials [22, 23].

4. THE ISSUE OF THE REPRODUCIBILITY OF THE PREPARATION OF THE SUPERHARD STABLE NANOCOMPOSITES

Because recently several workers have questioned the validity of our results [37, 39] and other had difficulties to reproduce them (see e.g. [40] and also references in [41]) it is appropriate to briefly discuss this issue. The questioning of the correctness of our hardness measurements in [37] was already clarified (see e. g. [24, 36, 42]). We have shown that a variety of artefacts may falsify the hardness measurements on superhard coatings. Particularly when measured by "nanoindentation" at a small applied load of ≤ 10 mN, too high values may be obtained by the load-depth-sensing technique [24, 36, 42]. Therefore, a variety of published data reporting very high hardness for ≤ 1 – 3 μm thin coatings may be incorrect. However, in our earlier (for a review see [11]) as well as in the recent [23, 24, 36, 38, 42] papers we have clearly explained that the load-independent (load range typically 30 to 150 mN) values of the high hardness reported by us on thick

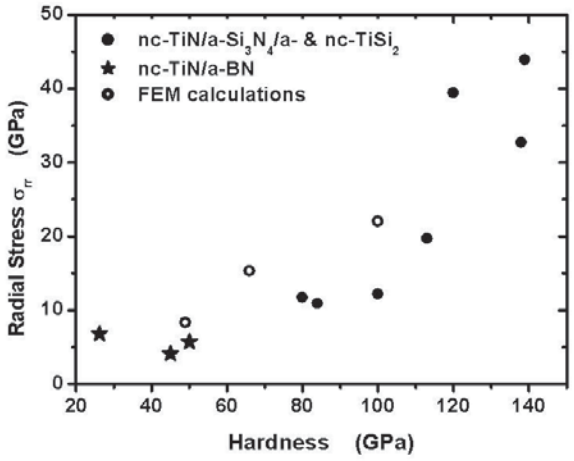

Fig. 5. Tensile stress which the coatings of the given hardness sustain without crack formation (see text).

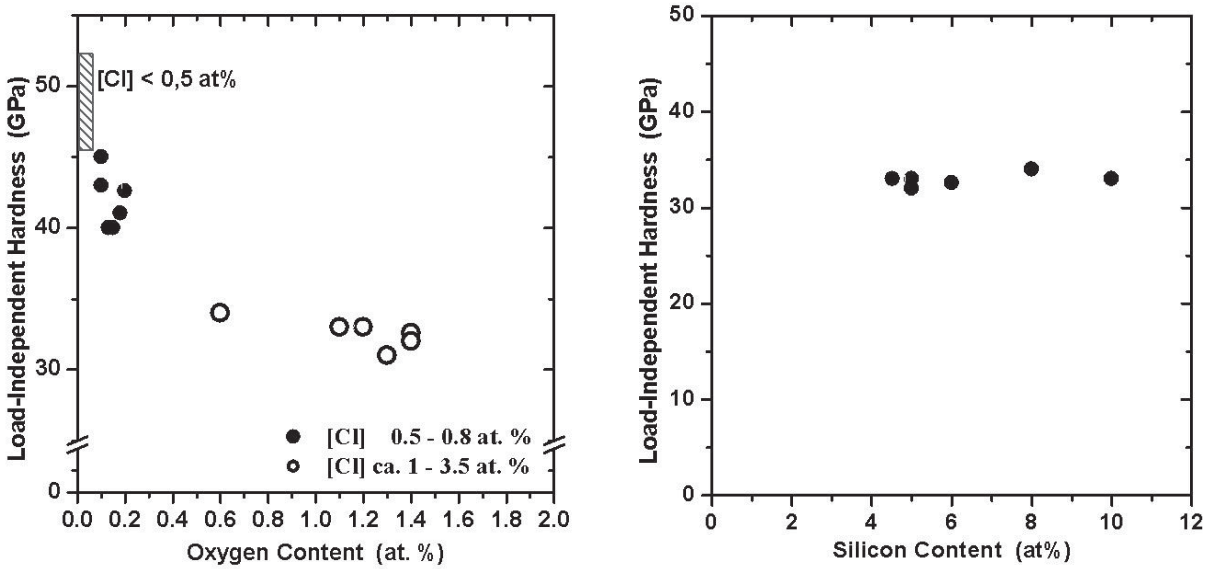

Fig. 6. a) Dependence of the hardness on oxygen impurity content for nc-TiN/a-Si_3N_4 nanocomposites with a low, medium and high chlorine content (see text). b) Hardness of the nc-TiN/a-Si_3N_4 nanocomposites with the highest oxygen impurities of 1 to 1.5 at.% versus the silicon content (see text).

coatings and verified by calibrated SEM are correct.

There are, however, several possible sources of errors that may make our results indeed difficult to reproduce. This can be either due to inappropriate choice of the deposition conditions that do not allow the system to achieve the stable nanostructure with the required sharp interface [4, 11 41] or to impurities [43]. Here we shall briefly summarize the most important findings that we achieved recently.

Already in our first paper on the generic design concept [4] we discussed the thermodynamic and kinetic conditions necessary for the formation of the nanocomposites with a stable nanostructure and sharp grain boundaries. Let us recall briefly: The strong (spinodal) phase segregation is thermodynamically driven, i. e. the nitrogen (we restrict ourselves here to the nitride systems) activity during the deposition must be sufficiently high. In simplified terms, the nitrogen partial pressure should be at least 10^{-2} mbar [4]. Because the phase spinodal segregation is diffusion controlled, the deposition temperature should be sufficiently high, typically ≥ 500 °C [49]. This has been recently confirmed by several research groups [45-47]. Therefore it is not surprising when Meng *et al*. [40] could not achieve any hardness enhancement because they were depositing under a too low nitrogen pressure of 10^{-4} mbar and a low temperature of ≤250 °C. This issue should be now sufficiently clear and understood.

Less known is the critical role of minor impurities in the coatings that can degrade their properties. Fig. 6a shows the detrimental effect of oxygen impurities in the binary nc-TiN/a-Si_3N_4 nanocomposites [43]. One notices that already impurities of 0.1 at.% of oxygen strongly decrease the achievable hardness and if they rise to ≥0.6 at.% the hardness remains limited to about ≤33 GPa. Furthermore, no hardness enhancement with increasing silicon content is observed in the coatings with the high impurity content (see Fig. 6b) in agreement with the report of Meng *et al.* who found only a monotonous decrease of the hardness from about 32 GPa to 24 when the silicon content was increased from 0 (pure TiN with hardness of 32 GPa !) to about 24 GPa for Ti-Si-N coatings with about 18 at.% of silicon. Notice, that in our nc-TiN/a-Si_3N_4, nc-W_2N/a-Si_3N_4 and nc-VN/a-Si_3N_4 coatings a maximum of the hardness of 45 – 55 GPa was found for Si-content of 7 – 9 at.% [4, 11, 48]. A similar effect plays also chlorine [43] and hydrogen [41]. We refer to our recent papers for further details.

5. INDUSTRIAL APPLICATION

The superhard nanocomposites were industrialized by the Czech company SHM Ltd. [26, 27, 31] using a specially designed vacuum arc evaporation with a

central cathode that provides the conditions needed for the formation of the stable nanostructure [32-34]. The nc-$(Al_{1-x}Ti_x)N$/a-Si_3N_4 nanocomposites are produced on large industrial scale as tribological coatings for cutting and forming tools. They are particularly suitable for dry and hard cutting operations (drilling, turning, milling). For interrupted cutting, such as milling, compositionally modulated 'multilayered' coatings show a much better performance than single layered ones [32-34, 44, 49].

More recently, SHM and the Swiss company PLATIT developed a new generation of advanced coatings industrial equipment that uses the new Lateral Rotating Arc Cathode (**LARC®**) which provides nc-$(Al_{1-x}Ti_x)N$/a-Si_3N_4 nanolayered nanocomposite coatings with a period of the compositional changes adjustable in the range of 7 to 10 nm, i. e. close to the optimum. This technology also uses the "**Virtual Shutter®**" for a simple but very efficient pre-cleaning of the cathodes which significantly improves the adhesion of the coatings and consequently the life time of the coated tools.

Fig. 7 shows as an example the number of holes drilled without any lubricants in a tough steel by means of a drill made of cemented carbide and coated with a variety of coatings. One notices that using the **LARC®** technology improves already the cutting performance of conventional coatings (e. g. TiN). The example ot the comparison of AlTiN (Al-rich $(Al_{1-x}Ti_x)N$) coatings deposited without and with the "**Virtual Shutter®**" illustrates the significant improvement by almost of a factor of 2. Finally, the last column shows that the cutting performance of the nanolayered, superhard nanocomposites nc-$(Al_{1-x}Ti_x)N$/a-Si_3N_4 is almost a factor of 4 better than the state-of-the art $(Al_{1-x}Ti_x)N$. Similar improvement was found in many other machining and forming operations.

These very new achievements illustrate the great potential of the superhard nanocomposite coatings in dry and minimum quantity lubricant ("MQL") machining. Because the costs of environmentally friendly recycling and disposal of the lubricants and coolants represent a significant part of total machining costs there is a strong trend towards dry or MQL machining. Therefore we expect a strong increase of the applications of these novel coatings in the near future. For further details see [31, 41,49,50].

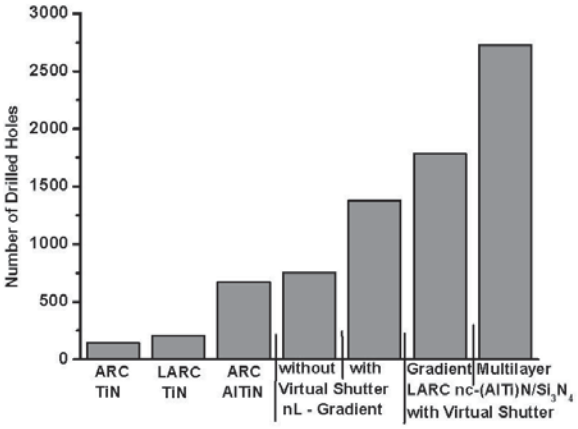

Fig. 7. Comparison of the cutting performance of conventional, state-of-the-art TiN and AlTiN coatings with the new ones prepared by means of the LARC coating technology (see text). Notice, that the nc-$(Al_{1-x}Ti_x)N$/a-Si_3N_4 nanocomposite coatings show an almost 4-times better performance than the state-of-the-art $(Al_{1-x}Ti_x)N$ coatings. Dry drilling of steel with 5 mm diameter drill made of cemented carbide with Corner Wear = 200 μm. The numbers indicate the total number of drilled holes [49].

ACKNOWLEDGEMENT

I would like to thank Dr. Maritza G. J. Veprek-Heijman for many useful comments to this manuscript. This work has been supported in part by the European Commission under Growth Programme in the frame of the 5th RTD Framework Programme under the contract number G5RD-CT-2000-0222 Project "NACODRY" and by the NATO SfP Project No. 972379 "Protection Coatings".

REFERENCES

[1] R. W. Hertzberg, *Deformation and Fracture Mechanics of Engineering Materials,* 3rd ed. (Wiley, New York, 1989).

[2] A. A. Griffith, In: *Proc. First Int. Congress Appl. Mech.*, ed. by C. B. Biezeno and J. M. Burgers (J. Waltman Jr., Delft, 1924) p. 55.

[3] A. Kelly and N. H. Macmillan, *Strong Solids* (Clarendon, Oxford 1986).

[4] S. Veprek and S. Reiprich // *Thin Solid Films* **268** (1995) 64.

[5] H. Männling, D. Patil, K. Moto, M. Jilek and S. Veprek // *Surf. Coat. Technol.* **146-147** (2001) 263.

[6] E. O. Hall // *Proc. Phys. Soc.* **B 64** (1951) 747.

[7] N. J. Petch // *J. Iron Steel Inst.* **174** (1953) 25.

[8] S. A. Barnet, In: *Physics of Thin Films*, Vol. **17**, *Mechanic and Dieletric Properties*, ed. by M. H. Francombe and J. L. Vossen (Academic Press, Boston, 1993) p. 2.

[9] R.A. Andrievski // *J. Solid State Chem.* **133** (1997) 249; *J. Mater. Sci.* **32** (1997) 4463.
[10] S. A. Barnet and A. Madan // *Phys. World* **11** (1998) 45.
[11] S. Veprek // *J. Vac. Sci. Technol.* **A 17** (1999) 2401.
[12] R. A. Andrievski // *Int. J. Refractory Metals & Hard Mater.* **19** (2001) 447.
[13] *Handbook of Deposition Technologies for Films and Coatings, 2nd ed.*, ed. by R. F. Bunshah (Noyes Publ. Park Ridge, 1994).
[14] S. Veprek, F.-A. Sarott and Z. Igbal // *Phys. Rev.* **B 36** (1987) 3344.
[15] J. Musil, S. Kadlec, J. Vyskocil and V. Valvoda // *Thin Solid Films* **167** (1988) 107.
[16] W. Herr and E. Broszeit // *Surf. Coat. Technol.* **97** (1997) 335.
[17] P. Karvánková, H.-D. Männling, C. Eggs and S. Veprek // Surf. Coatings *Technol.* **146-147** (2001) 280.
[18] J. Musil // *Surf. Coat. Technol.* **125** (2000) 322.
[19] S. Veprek, P. Karvankova, J. Prochazka, H. Männling and M. Jilek // *MRS Symp. Proc.* **697** (2002) 27.
[20] H. Schmalzried, *Chemical Kinetics of Solids* (VCH Verlag, Weinheim, 1995).
[21] A. R. West, *Solid State Chemistry and its Applications* (J. Wiley & Sons, Chichester, 1984).
[22] A. S. Argon and S. Veprek, In: *Proc. 22nd Riso Int. Symp. on Materials Science: Science of Metastable and Nanocrystalline Alloys, Structure, Properties and Modeling*, ed. by A. R. Dinesen, M. Eldrup, D. Juul Jensen *et al.*, (Riso Nat. Laboratory, Roskilde, Denmark, 2001) p. 183.
[23] S. Veprek and A. S. Argon // *J. Vac.Sci. Technol.* **B 20** (2002) 560.
[24] S. Veprek, S. Mukherjee, P. Karvankova, H.-D. Männling, J. L. He, K. Moto and A. S. Argon // *J. Vac. Sci. Technol.* **A 21** (2002) 532.
[25] A. Niederhofer, P. Nesladek, H.-D. Männling, K. Moto, S. Veprek and M. Jilek // *Surf. Coatings Technol.* **120-121** (1999) 173.
[26] P. Holubar, M. Jilek and M. Sima // *Surf. Coatings Technol.* **133-134** (2000) 145.
[27] T. Cselle, P. Holubar, M. Jilek and M. Morstein, *Int. Conf. On Metallurgical Coatings and Thin Films*, San Diego April 2002, paper No. G4-2-3.
[28] H. Ljungcrabtz, L. Hultman, J.-E. Sundgren and L. Karlson // *J. Appl. Phys.* **78** (1995) 832.
[29] L. Hulman // *Vacuum* **57** (2000) 1.
[30] S. Veprek, A. Niederhofer, K. Moto, P. Nesladek, H. Männling and T. Bolom // *Mater. Res. Soc. Symp. Proc.* **581** (2000) 321.
[31] SHM Ltd., CZ-78803 Novy Malin, Novy Malin 266; E-mail: shm@shm-cz.cz
[32] P. Holubář, M. Jílek and M. Šíma // *Surf. Coat. Technol.* **120-121** (1999) 184.
[33] S. Veprek, P. Nesladek, A. Niederhofer, F. Glatz, M. Jilek and M. Sima // *Surf.Coat. Technol.* **108-109** (1998) 138.
[34] S. Veprek and M. Jilek // *Vacuum* **67** (2002) 443.
[35] S. Veprek, H.-D. Männling, M. Jilek and P. Holubar, manuscript in preparation, to be published.
[36] S. Veprek, S. Mukherjee, P. Karvankova, H.-D. Männling, J. L. He, J. Xu, J. Prochazka, A. S. Argon, A. S. Li, Q. F. Fang, S. Z. Li, M. H. Manghnani, S. Tkachev and P. Zinin // *Mater. Res. Soc. Symp. Proc.* **750** (2003) 9.
[37] J. Musil, H. Zeman, F. Kunc and J. Vlcek // *Mater. Sci. Eng.* **A 340** (2002) 281.
[38] S. Veprek, S. Mukherjee, H.-D. Männling and J. L. He // *Mater. Sci. Eng.* **A 340** (2002) 292.
[39] Anonymous referee of our paper [27].
[40] W.J. Meng, X. D. Zhang, B. Shi, R. C. Tittsworth, L. E. Rehn and P. M. Baldo // *J. Mater. Res.* **17** (2002) 2628.
[41] J. Prochazka and S. Veprek, manuscript in preparation; to be published.
[42] S. Veprek, S. Mukherjee, P. Karvankova, H.-D. Männling, J. L. He, K. Moto and S. Argon, *Invited Lecture at the Int. Conf. on Metalurgical Coatings and Thin Films*, San Diego April 2002 // *Thin Solid Films* **436** (2003) 220.
[43] S. Veprek, H.-D. Männling, A. Niederhofer, D. Ma and S. Mukherjee, manuscript in preparation; to be published.
[44] M. Jilek, T. Cselle, P. Holubar, M. Morstein, M. G. J. Veprek-Heijman and S. Veprek // *Plasma Chem. Plasma Processing*, (2004) submitted.
[45] F. Vaz, L. Rebouta, S. Ramos, M. F. da Silva and J. C. Soares // *Surf. Coat. Technol.* **198-109** (1998) 236.

[46] F. Vaz, L. Rebouta, P. Godeau, J. Pacaud, H. Garem, J. P. Riviere, A. Cavaleiro and E. Alves // *Surf. Coat. Technol.* **133-134** (2000) 307.
[47] S.H. Kim, J. K. Kim and K. H. Kim // *Thin Solid Films* **420-421** (2002) 360.
[48] S. Veprek, M. Haussmann and S. Reiprich // *J. Vac. Sci. Technol.* **A 14** (1996) 46.
[49] M. Jilek, P. Holubar. M. G. J. Veprek-Heijman and S. Veprek // *MRS Symp. Proc.* **750** (2003) 393.
[50] T. Cselle // *Werkzeug Technik* **77** (2003, March) 52; http://www.platit.ch.